Available online at www.sciencedirect.com
ScienceDirect
Carbohydrate Research 342 (2007) 819–825
Carbohydrate RESEARCH

Innovative crystal transformation of dihydrate trehalose to anhydrous trehalose using ethanol

Tetsuya Ohashi,[a,b] Hidefumi Yoshii[a,*] and Takeshi Furuta[a]

[a]*Department of Biotechnology, Tottori University, Koyama Minami 4-101, Tottori 680-8552, Japan*
[b]*Production Technology Development, Hayashibara Co., Ltd, 7-7 Amase Minamimachi, Okayama 700-0834, Japan*

Received 11 November 2006; received in revised form 22 December 2006; accepted 9 January 2007
Available online 14 January 2007

Abstract—The crystal transformation of dihydrate trehalose to anhydrous trehalose was investigated using ethanol and a new type of crystal particle with porous structure could be obtained. The specific surface area of the anhydrous crystal transformed at 50 °C was 3.3 m^2/g, with a median pore diameter of 0.21 μm, and void volume of 0.22 mL/g. The crystal transformation was monitored by measuring the crystal moisture content. The crystal transformation rates could be correlated with the Avrami equation, using the mechanism parameter $n = 11.5$, suggesting that the change of surface area occurred during crystal transformation from dehydrate to anhydrous trehalose. The apparent activation energy of the crystal transformation was 132 kJ/mol.

Keywords: Dihydrate trehalose; Anhydrous trehalose; Crystal transformation; Ethanol

1. Introduction

α,α-Trehalose (α-D-glucopyranosyl α-D-glucopyranoside) is a non-reducing disaccharide found in many organisms[1] where its primary roles are as an energy source and protection of living cells, proteins, and phospholipids from the damage caused by dryness by changing into various crystalline forms.[2–5] Since trehalose is also present at low concentration in various food, we continually ingest this sugar as part of a daily diet. For example, trehalose is used in bakery products, confectionery, cereals, rice, noodle, beverages, frozen food, and dried food. The main purposes for using trehalose are lowering of sweetness (about 45% as sweet as sucrose), moisture retention, prevention of starch retrogradation, protection of food ingredients, and improvement of preservation stability.

Trehalose has started to gain acceptance throughout the world as a food additive. In 1995, Hayashibara Co. Ltd, Okayama, Japan, succeeded for the first time in producing trehalose directly from starch via an enzymatic reaction.[6–9] Nowadays about 30,000 ton of trehalose is used annually in the food and cosmetic industries in Japan.

Trehalose crystals exist in the dihydrate and polymorphic anhydrous crystalline forms, which exhibit complicated polymorphism depending on the given thermodynamic conditions. Dihydrate trehalose (T_h) is stable under normal environmental conditions and can be easily obtained by crystallization from supersaturated solutions. Dehydration of dihydrate trehalose generates four kinds of polymorphic crystalline forms of anhydrous trehalose—α-, β-, γ-, and ε-forms. Many studies have reported phase transitions occurring during the heating process of trehalose dihydrate using X-ray diffraction (XRD), differential scanning calorimetry (DSC) and thermogravimetry–differential analysis (TG–DTA) etc.[10–13]

Abbreviations: XRD, X-ray powder diffraction; SEM, scanning electron microscopy; DSC, differential scanning calorimetry; T_h, dihydrate trehalose; T_α, α-form of anhydrous trehalose; T_β, β-form of anhydrous trehalose; T_γ, γ-form of anhydrous trehalose; T_ε, ε-form of anhydrous trehalose

* Corresponding author. Tel.: +81 857 31 5272; fax: +81 857 31 0881; e-mail: foodeng.yoshii@bio.tottori-u.ac.jp

0008-6215/$ - see front matter © 2007 Elsevier Ltd. All rights reserved.
doi:10.1016/j.carres.2007.01.008

The β-form of anhydrous trehalose (T_β) has been thoroughly characterized with a known crystal structure. T_β is a less hygroscopic stable anhydrous crystalline form and is obtained by heating T_h or other metastable anhydrous forms. Sussich et al.[11] have reported thermal analysis data showing the existence of several polymorphs of anhydrate trehalose. They obtained T_β by using scan rates varying between 1 and 60 °C/min with DSC. Taylor and York[14] measured large particles (>425 μm) underwent a solid–solid conversion from T_h to T_β at a temperature as low as 80 °C. The α-form (T_α) that exists at the melting point around 130 °C was obtained after exposing dihydrate trehalose (<63 μm) to 0% relative humidity (RH) at 25 °C,[15] and also by vacuum drying for 48 h at 50 °C.[16] A new crystalline form called T_γ is a mixture of the T_h and the T_β. T_h is considered as existing at the center of the crystal and encapsulated by T_β.[12] Another new unidentified crystalline form called T_ε has recently been obtained in a calorimeter by heating T_h from room temperature to 220 °C under wet nitrogen gas.[13]

Many research studies have been carried out on the protective function and crystal transformation of trehalose. However, research on the physical conformational changes of trehalose by crystal conversion has not been reported. In this study, an innovative process to produce anhydrous crystal of trehalose with fine porosity using ethanol as the dehydration medium was explored. Anhydrous crystals with fine porous structure could be obtained.

2. Results and discussion

2.1. Crystal transformation with the solvent method

Figure 1 shows the crystal transformation behavior of the dihydrate trehalose crystal to the anhydrous one described by means of the changes in moisture content. The dehydration process was performed at 50, 60, and 70 °C. Unique dehydration curves of dihydrate trehalose were obtained by this method. The dehydration process had lag times before the moisture content of the sample started to decrease. During the lag time the moisture content of trehalose remained at around 9.5 ± 0.2%. After the lag time, the moisture of the crystal abruptly decreased to a terminal value of around 0.5%. Changes in the moisture content of crystal trehalose over time were typical sigmoid curves, dependent on the temperature of the dehydration medium, ethanol. These crystal transformation curves could not be correlated with the Avrami equation using the typical value of $n = 3$–4, but were well correlated when $n = 11.5$ was used, as shown by the solid lines in Figure 1.[17] The crystal transformation process involves many steps including the change of surface area by the pore formation. We assume that the rate-limiting steps might comprise the dehydration of crystallization water from dihydrate trehalose forming amorphous trehalose, which is a surface area-dependent reaction. The apparent rate constant might be in proportion to the pore formation. Thus, the expansion of surface area of trehalose crystal due to pore formation entails a great increase in the n value. The apparent rate constant might be in proportion to the pore formation. The Arrhenius plot for the apparent rate constants k of the crystal transformation is shown in Figure 2. The values of k were well correlated, and the apparent activation energy obtained was 132 kJ/mol. Sussich et al.,[18,19] indicated that the enthalpy change in water evaporation from dihydrate trehalose to amorphous trehalose was 113.5 kJ/mol at 100 °C. Taylor and York have measured the activation energy of the crystal transformation by monitoring the isothermal dehydration using TGA.[20] At temperatures between 40 and 60 °C, the activation energy was 55–56 kJ/mol for the larger sized (>425 μm) crystal particles,

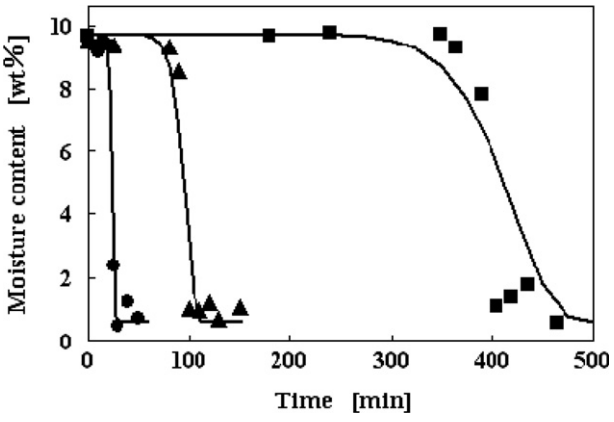

Figure 1. Time courses of crystal moisture content. The solid lines were calculated using the Avrami equation. Dehydration at 70 °C (●), 60 °C (▲), and 50 °C (■).

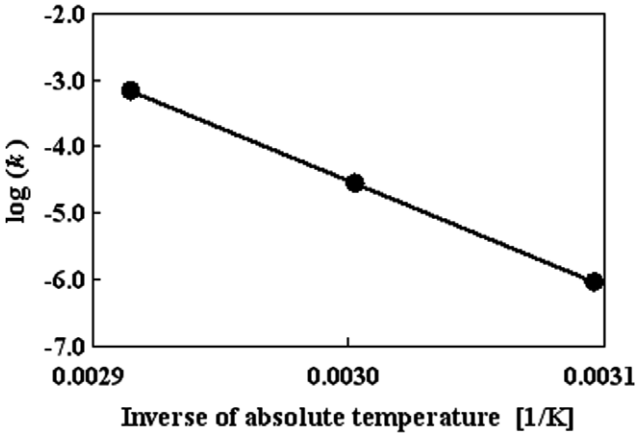

Figure 2. The Arrhenius plot of the crystal transformation rate constant by the Avrami equation.

41–42 kJ/mol for the smaller sized (<45 μm) particles, and 50–51 kJ/mol for the unfractionated crystal particles. The apparent activation energy of the crystal transformation in the present work is around two times higher than the values reported by Taylor and York. It should be noted that in a diffusion-controlled process, the activation energy generally falls in the range of 8–10 kJ/mol, while in an integration-controlled process, it is above 40 kJ/mol.[21] The larger apparent activation energy in the present work may include the drastic structural changes in the crystal lattice during formation of the β-form of anhydrous trehalose in ethanol.

2.2. Anhydrous crystalline form

Figure 3 shows the X-ray diffractometry of dihydrate trehalose (A), anhydrous trehalose by the ethanol method (B) and vacuum drying method (C). Angles and characteristic diffraction peaks of the dihydrate and anhydrous crystals are also shown in Figure 3. The degrees of crystallinity of each crystal by the Ruland method were 82.5% for (A), 81.4% for (B) at 50 °C, and 84.0% for (C). X-ray diffractograms for (B) and (C) show almost a similar pattern. These X-ray diffractograms were identified as similar to that of the T_β crystalline form, which is the stable anhydrous form. In the case of (C), the characteristic diffraction peaks of dihydrate trehalose crystal ($2\theta = 8.7°$ and 23.8°) also appeared as surrounded by the dotted line circle. Presumably, dehydration by vacuum drying was not complete. DSC curves of dihydrate crystals and anhydrous crystals by vacuum drying and by the ethanol method are shown in Figure 4. Both anhydrous crystals showed similar endothermic peaks at around 197 °C due to the melting of the crystals. The anhydrous crystal obtained by vacuum drying showed another endothermic peak at around 93 °C due to the melting of the hydrous crystals. They were both identified as the anhydrous crystal form T_β by X-ray powder diffractogram. However, the temperature of the endothermic peak was lower than 200 °C reported in some literatures for the anhydrous crystal form T_β.[14,15,18] Although the reason for this difference is unknown at present, it may be due to a small amount of moisture or the influence of purity. The enthalpy change in melting was 54.4 kJ/mol for the anhydrous crystals obtained by the ethanol method and 54.8 kJ/mol for those obtained by vacuum drying. These enthalpy changes were close to the values reported by Sussich et al.[11]

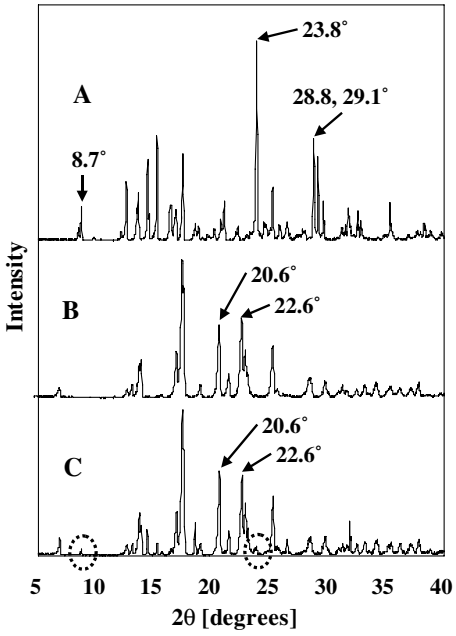

Figure 3. X-ray diffraction patterns of trehalose: (A) hydrous crystal from solution, (B) anhydrous crystal transformed by the ethanol method, and (C) anhydrous crystal transformed by vacuum drying.

2.3. Characteristics of particle structure

SEM photographs of the dihydrate crystals (A–C), anhydrous trehalose obtained by the ethanol method (D–F) and by vacuum drying (G–I) are shown in Figure 5. The dihydrate crystal is a single rectangular crystal. It has a smooth surface, clearly visible sides and edges (Fig. 5A). Figure 5B and C show the magnified crystal surface with small crystals adhered onto the smooth surface. The anhydrous crystals obtained by vacuum drying had no visible sides and edges (Fig. 5G). As shown in Figure 5I, the surface of the crystal is covered with small irregular shaped crystals with slightly fine openings that may not have extended to the inside. On the other hand, for anhydrous crystals dehydrated by the ethanol method, the sides and the edges are not clear (Fig. 5D) analogous to that by vacuum drying. The surface is visible as

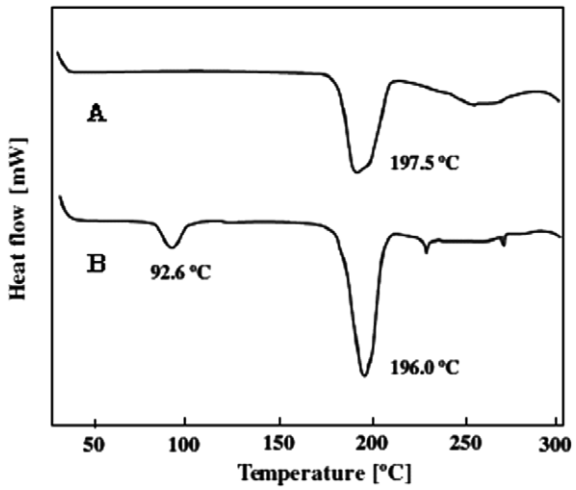

Figure 4. DSC thermograms of anhydrous trehalose: (A) anhydrous crystal transformed by the ethanol method and (B) anhydrous crystal transformed by vacuum drying.

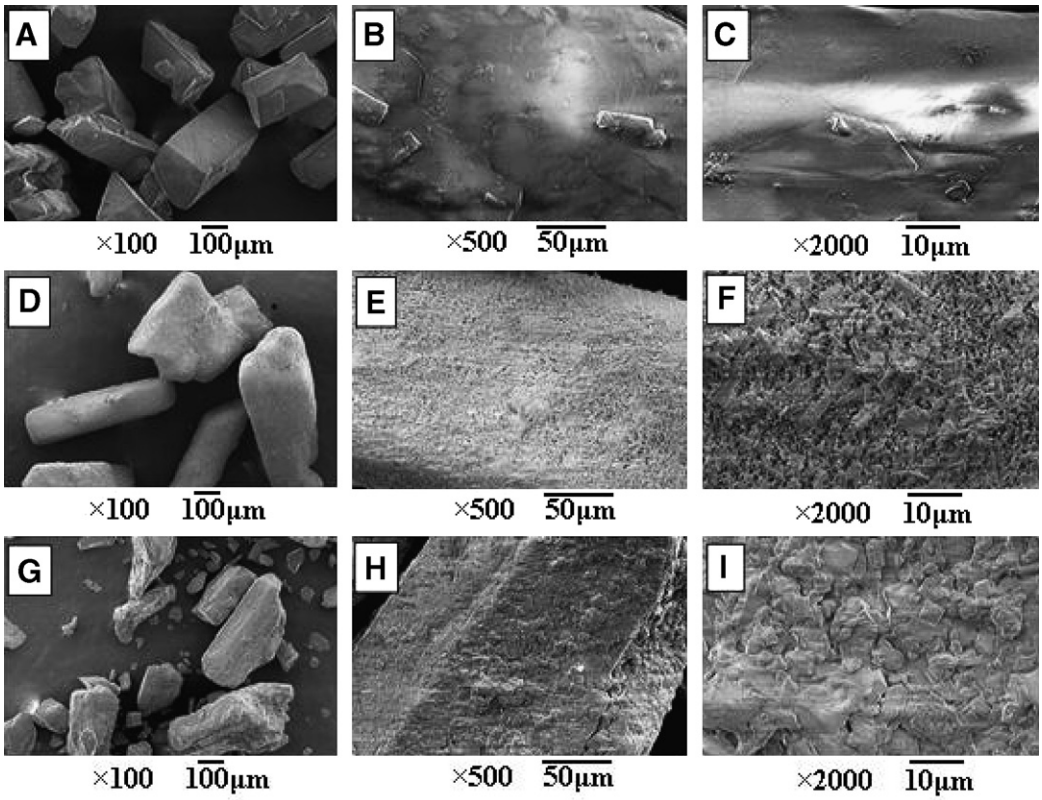

Figure 5. SEM photomicrographs of anhydrous trehalose: (A)–(C) dihydrate crystal from solution, (A) ×100, (B) ×500, (C) ×2000, (D)–(F) anhydrous crystal transformed by the ethanol method, (D) ×100, (E) ×500, (F) ×2000, (G)–(I) anhydrous crystal transformed by vacuum drying, (G) ×100, (H) ×500, and (I) ×2000.

a melt done, but the original shape of the particle before dehydration remains (Fig. 5E). As is clearly shown in Figure 5F, the surfaces of these crystals are covered with enormous number of fine columnar crystals forming pores that may extend to the inside of the particle.

2.4. Characteristics of fine structure

The pore size distribution and differential intrusion volume, measured with a mercury porosimeter, are shown in Figure 6. As illustrated in Figure 6, the anhydrous crystals obtained by the ethanol method have a higher cumulative intrusion volume than those obtained by vacuum drying. Also, pores that measure from 0.01 to 1.0 μm in diameter have markedly higher differential intrusion than those obtained by vacuum drying. Table 1 summarizes the pore characteristics estimated from Figure 6 for anhydrous crystals obtained by the ethanol method and vacuum drying. For the anhydrous crystals obtained by the ethanol method, the specific surface area was 2.5–3.3 m^2/g, which was 5–8 times greater, and the intrusion volume of 0.22–0.28 mL/g was 7–9 times greater than that for anhydrous trehalose by vacuum drying. The median pore diameter was also finer for anhydrous trehalose obtained by the ethanol method. The median pore diameter of 0.21–0.29 μm was comparable to that estimated from the SEM photographs in Figure 5F. The higher values of the specific surface area and the intrusion volume indicated that the physical structure of the crystal particle obtained by the ethanol method might have formed a three-

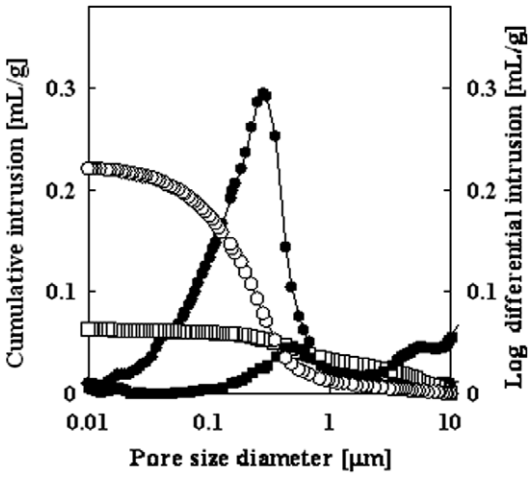

Figure 6. Cumulative and differential intrusions of anhydrous trehalose from the ethanol dehydration method at 50 °C. Vacuum drying differential intrusion (■), vacuum drying cumulative intrusion (□), ethanol method differential intrusion (●), ethanol method cumulative intrusion (○).

Table 1. Characteristics of anhydrous trehalose crystal

Dehydration method	Surface area (m^2/g)	Median pore diameter (μm)	Intrusion volume (mL/g)
Ethanol method at 50 °C	3.31	0.21	0.22
Ethanol method at 70 °C	2.51	0.29	0.28
Vacuum drying	0.47	0.40	0.03

dimensional network, but not for that obtained by vacuum drying.

Surana et al.[22] reported that the specific surface area was $0.25 \pm 0.10\ m^2/g$ for dehydrated amorphous trehalose (particle size: 30–50 μm) and $1.02 \pm 0.22\ m^2/g$ for spray-dried amorphous trehalose (particle size: 2–4 μm). Comparison of these results revealed that the anhydrous crystal obtained by the ethanol method had a remarkably larger surface area even though the crystal particle size was small.

2.5. Changes in the crystal surface morphology during dehydration by the ethanol method

Figure 7 shows the SEM photographs of trehalose crystals during crystal transformation by the ethanol method at 60 °C. The surface morphology was changing during the lag time even though the moisture content hardly changed. The luster of the crystal disappeared after 25 min of reaction time and a projection was

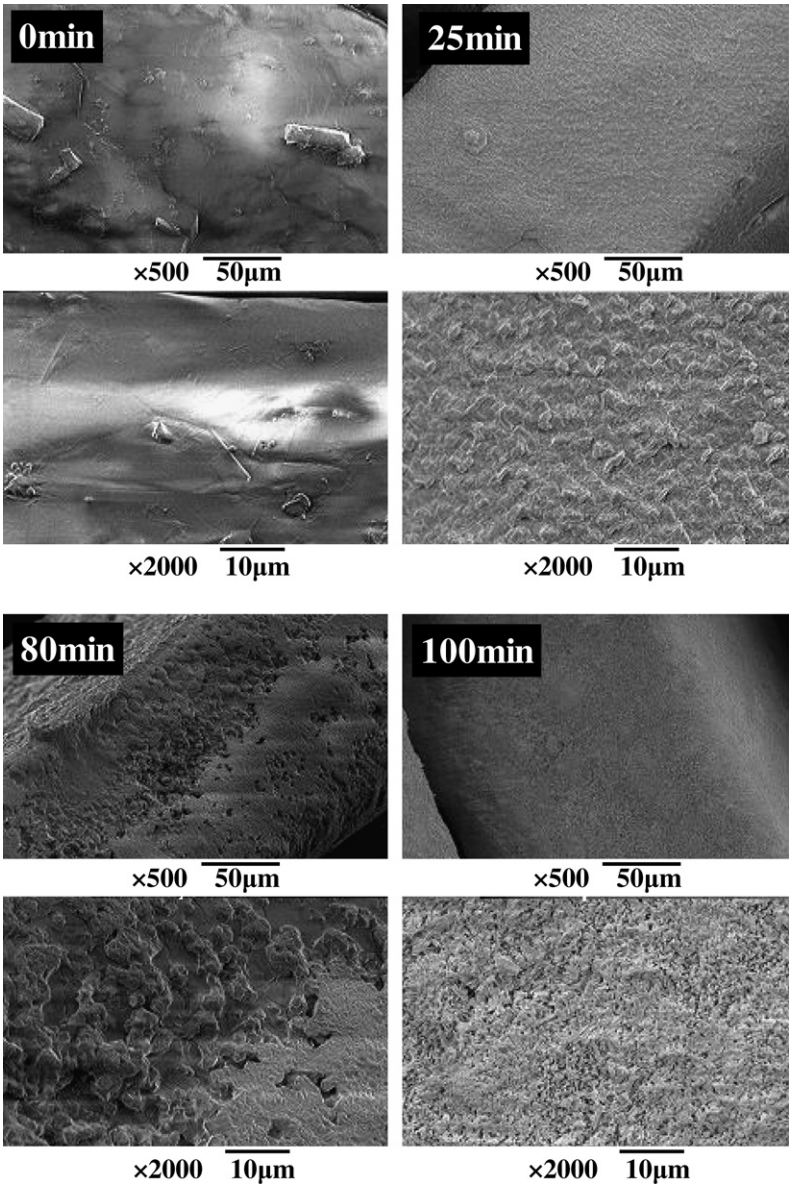

Figure 7. SEM photomicrographs of the surface morphology of the trehalose crystal during crystal transformation at 60 °C. Initial dihydrate crystal appeared in 0 min, during lag time in 25 min; rapid dehydration started at 80 min and ended at 100 min.

observed on the surface. The crystal surface turned rougher gradually and eventually developed into a surface that resembled mass-like rocks at 80 min when rapid dehydration started. A three-dimensional pore structure was formed within a micrometer sized crystal at 100 min, when dehydration almost ended. The mechanism of crystal transformation could be postulated as follows on the basis of the experimental data and the above discussion: At the beginning, the surface of the dihydrate crystal was dehydrated by ethanol and a thin amorphous layer was formed on the surface of the crystal. Then, the water molecules from the inner layer of the crystal were freed and moved outwardly through the amorphous layer to the outer environment causing the thickness of the amorphous layer to expand inwardly. When moisture and mobility of the amorphous layer reached a level sufficient for crystal nucleation, the anhydrous crystals grew and rapid crystallization started. McGarvey et al.[23] reported that the glass transition point (normally around 120 °C at 0% moisture content) decreased by about 14 °C with an increase of 1% moisture content. Therefore, the moisture content and water mobility in trehalose crystal may influence the mechanism of crystal transformation.

3. Experimental

3.1. Materials

Ethanol (purity above 99.8%) was obtained from Nihon Alcohol Distribution Co., Ltd (Tokyo, Japan). Dihydrate trehalose and vacuum dried anhydrous crystal trehalose from Hayashibara Co., Ltd (Okayama, Japan) were used. The purity of the dihydrate trehalose crystals was 99.3% with a 9.7% moisture content and median particle diameter of about 380 μm (Rosin-Rammler size parameter: 417 μm; exponential parameter: 4.20).

3.2. Physical methods

3.2.1. Dehydration by the ethanol method. The crystal dehydration apparatus using ethanol as a dehydration medium is shown in Figure 8. Experiments were carried out in a 2000 mL glass reactor (reaction flask, cylindrical round bottom with groove, Shibata Scientific Technology Ltd, Tokyo, Japan) equipped with a turbine blade agitator (three-one motor, Model BL600, Shinto Scientific Co., Ltd, Tokyo, Japan). Approximately 1200 mL of ethanol was pre-heated to various temperatures in a water bath to which 120 g of dihydrate trehalose crystals was added. The mixture was then agitated at about 170 rpm at 50, 60, or 70 °C. One twentieth to one tenth of a liter of the reaction mixture (slurry) was aspirated into a sampling vessel and immediately separated with a basket type centrifuge (Model SYK-3800-15A, Sanyo Rikagakukikai Seisakysho, Co., Ltd, Tokyo, Japan). An interval of no longer than 30 s was allowed between the sampling and the start of centrifugation. Wet crystals were thinly spread in a stainless container pre-heated to 50 °C, and dried for 20 min in a ventilation dryer (Model FV-630, Toyo Seisakusho Co., Ltd, Tokyo, Japan) at 50 °C in order to remove the residual ethanol.

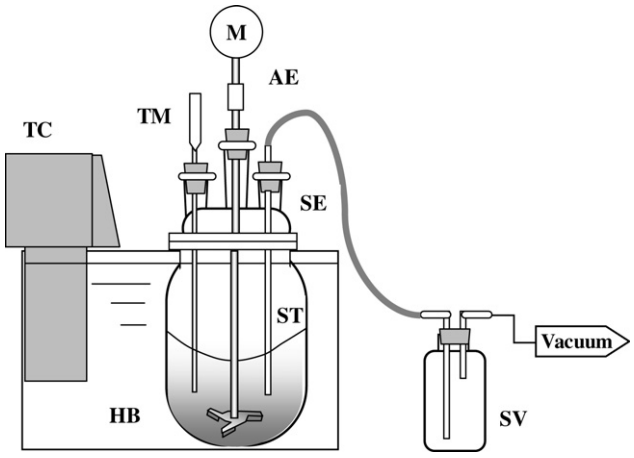

Figure 8. Schematic diagram of crystal transformation by the ethanol method: SF, separable flask; HB, water bath; ST, sampling tube; TM, thermometer; AE, agitation equipment; TC, temperature control unit; SV, sampling vessel.

3.2.2. Moisture content analysis. Moisture content was determined using a Karl Fischer titrimeter (Model MK-SS, Kyoto Electronics Manufacturing Co., Kyoto, Japan). About 100 mg of the trehalose sample was dissolved in the dehydrated solvent and titrated with a volumetric reagent (Solvent FM, Titrant SS 3 mg, Mitsubishi Chemical Co., Tokyo, Japan).

3.2.3. X-ray powder diffractometry (XRD). The trehalose crystals were pounded in a mortar and filled in a sample holder of an aluminum plate for exposure to Cu-Kα radiation in a powder X-ray diffractometer (Model RAD-II B, Rigaku Co., Tokyo, Japan). Samples were scanned at a scanning speed of 3°/min over a diffraction angular range of 3–140° and the crystallinity of the sample was estimated by the Ruland method.[24]

3.2.4. Thermal analysis. Thermal analysis was performed with a differential scanning calorimeter (Model DSC8230, Rigaku Co., Tokyo, Japan). About 6 mg of trehalose crystals was packed in an aluminum pan and heated at a rate of 10 °C/min from 30 to 310 °C.

3.2.5. Scanning electron microscopy (SEM). Scanning electron microscopy (Model JSM 6060, JEOL Co., Ltd, Tokyo, Japan) was used to investigate the microstructural properties of trehalose crystals. The trehalose

crystals were placed on a double-sided adhesive tape (Nisshin EM Co., Ltd, Tokyo, Japan) adhered to a SEM stub. All the samples were analyzed at an acceleration voltage of 2.0 kV.

3.2.6. Specific surface area analysis. Specific surface area of the trehalose crystals was determined by the Brunnauer, Emmet, and Teller (BET) method using a surface area analyzer (ASAP-2400, Micrometrics, Georgia, USA). As a pretreatment, trehalose crystals were degassed under vacuum at 40 °C for 15 h and about 3 g of sample was used for measurements.

3.2.7. Pore size analysis. Pore size distribution, pore diameter, and intrusion volume were measured by a mercury porosimeter (Autopore 9520 mercury porosimeter, Georgia, USA). About 0.5 g of sample was set in the measurement cell and mercury filling pressure was started from 15 kPa.

3.2.8. Particle size distribution. Particle size distribution was determined by the sieve fractionation method using standard sieves (JIS Z 8801). Three grams of the trehalose crystal particles was passed through a set of sieves of known aperture sizes. The sieves were mechanically vibrated for a fixed period of time. The weight of particles retained on each sieve was measured and the Rosin-Rammler distribution function was used to determine the median diameter.

3.3. Kinetic analysis of crystal transformation

The degree of crystal transformation ϕ_c was defined by the equation below:

$$\phi_c = (m_d - m)/(m_d - m_a) \quad (1)$$

where m is the moisture content of trehalose. m_d and m_a are the moisture content of dihydrate trehalose and anhydrous trehalose, respectively. In this experiment, m_d and m_a were 9.7% and 0.6%, respectively, because the moisture content of anhydrous trehalose had scattered values between 0.2% and 0.6%. For different crystal growth and different shapes of the nucleus, the generalized Avrami equation[17] below is applied to estimate the crystal transformation rate:

$$\phi_a = 1 - \phi_c = \exp[-(kt)^n] \quad (2)$$

where ϕ_a is the fraction of dihydrate trehalose to total trehalose, ϕ_c the crystal conversion from dihydrate trehalose to anhydrous trehalose, k the rate constant of crystal conversion, t reaction time under isothermal conditions, and n the mechanism parameter of crystal conversion. Both k and n depend on the nucleation and growth mechanisms. Usually at isothermal crystal growth, n is the value between 1 and 4. When crystal transformation occurred with the growth of solid sheaf under thermal conditions, n is larger than 6. Since the crystal transformation by the ethanol method seems to be coupled with changes of the surface area during crystal transformation, the value of n became much higher than that for the normal crystal transformation.

References

1. Oku, K.; Sawatani, I.; Chaen, H.; Fukuda, S.; Kurimoto, M. *Nippon Shokuhin Kagaku Kogaku Kaishi* **1998**, *45*, 381–384.
2. Yoshii, H.; Furuta, T.; Kudo, J.; Linko, P. *Biosci. Biotechnol. Biochem.* **2000**, *64*, 1147–1152.
3. Suzuki, T.; Imamura, K.; Yamamoto, K.; Sato, T.; Okazaki, M. *J. Chem. Eng. Jpn.* **1997**, *30*, 609–613.
4. Crowe, L. M. *Comp. Biochem. Physiol. Part A* **2002**, *131*, 505–513.
5. Patist, A.; Zoerb, H. *Biointerfaces* **2005**, *40*, 107–113.
6. Maruta, K.; Nakada, T.; Kubota, M.; Chaen, H.; Sugimoto, T.; Kurimoto, M.; Tsujisaka, Y. *Biosci. Biotechnol. Biochem.* **1995**, *59*, 1829–1834.
7. Nakada, T.; Maruta, K.; Tsusaki, K.; Kubota, M.; Chaen, H.; Sugimoto, T.; Kurimoto, M.; Tsujisaka, Y. *Biosci. Biotechnol. Biochem.* **1995**, *59*, 2210–2214.
8. Nakada, T.; Maruta, K.; Mitsuzumi, H.; Kubota, M.; Chaen, H.; Sugimoto, T.; Kurimoto, M.; Tsujisaka, Y. *Biosci. Biotechnol. Biochem.* **1995**, *59*, 2215–2218.
9. Sugimoto, T. *Shokuhin Kogyo* **1995**, *38*, 34–39.
10. Sussich, F.; Urbani, R.; Cesàro, A. *Carbohydr. Lett.* **1997**, *2*, 403–408.
11. Sussich, F.; Urbani, R.; Princivalle, F.; Cesàro, A. *J. Am. Chem. Soc.* **1998**, *120*, 7893–7899.
12. Sussich, F.; Princivalle, F.; Cesàro, A. *Carbohydr. Res.* **1999**, *322*, 113–119.
13. Furuki, T.; Kishi, A.; Sakurai, M. *Carbohydr. Res.* **2005**, *340*, 429–438.
14. Taylor, L. S.; York, P. *J. Pharm. Sci.* **1998**, *87*, 347–355.
15. Jones, M. D.; Hooton, J. C.; Dawson, M. L.; Ferrie, A. R.; Price, R. *Int. J. Pharm.* **2006**, *313*, 87–98.
16. Akao, K.; Okubo, Y.; Asakawa, N.; Inoue, Y.; Sukurai, M. *Carbohydr. Res.* **2002**, *334*, 233–241.
17. Chao, C. H.; Lu, H. Y. *Mater. Sci. Eng. A* **2000**, *282*, 123–130.
18. Sussich, F.; Bortoluzzi, S.; Cesàro, A. *Thermochim. Acta* **2002**, *391*, 137–150.
19. Sussich, F.; Cesàro, A. *J. Therm. Anal. Calorim.* **2000**, *62*, 757–768.
20. Taylor, L. S.; York, P. *Int. J. Pharm.* **1998**, *167*, 215–221.
21. Kim, K. J.; Kim, K. M. *Powder Technol.* **2002**, *122*, 46–53.
22. Surana, R.; Pyne, A.; Suryanarayanan, R. *Pharm. Res.* **2004**, *21*, 1167–1176.
23. McGarvey, O. S.; Kett, V. L.; Craig, D. Q. M. *J. Phys. Chem. B* **2003**, *107*, 6614–6620.
24. Ruland, B. W. *Acta Crystallogr.* **1961**, *14*, 1180–1185.